Chemistry A European Journal

Accepted Article

Title: Electrochemical Diselenation of BODIPY Fluorophores for Bioimaging Applications and Sensitization of 1O2

Authors: Ícaro A. O. Bozzi, Luana A. Machado, Emilay B. T. Diogo, Fábio G. Delolo, Luiza O. F. Barros, Gabriela A. P. Graça, Maria H. Araujo, Felipe T. Martins, Leandro F. Pedrosa, Lilian C. da Luz, Emmanuel S. Moraes, Fabiano S. Rodembusch, João S. F. Guimarães, André G. Oliveira, Sebastian Röttger, Daniel B. Werz, Cauê P. Souza, Felipe Fantuzzi, Jianhua Han, Todd B. Marder, Holger Braunschweig, and Eufrânio Nunes da Silva Júnior

This manuscript has been accepted after peer review and appears as an Accepted Article online prior to editing, proofing, and formal publication of the final Version of Record (VoR). The VoR will be published online in Early View as soon as possible and may be different to this Accepted Article as a result of editing. Readers should obtain the VoR from the journal website shown below when it is published to ensure accuracy of information. The authors are responsible for the content of this Accepted Article.

To be cited as: *Chem. Eur. J.* **2023**, e202303883

Link to VoR: https://doi.org/10.1002/chem.202303883

WILEY▪VCH

RESEARCH ARTICLE

Electrochemical Diselenation of BODIPY Fluorophores for Bioimaging Applications and Sensitization of $^1O_2$

Ícaro A. O. Bozzi,[a]+ Luana A. Machado,[a,h]+ Emilay B. T. Diogo,[a] Fábio G. Delolo,[a] Luiza O. F. Barros,[a] Gabriela A. P. Graça,[a] Maria H. Araujo,[a] Felipe T. Martins,[b] Leandro F. Pedrosa,[c] Lilian C. da Luz,[d] Emmanuel S. Moraes,[e] Fabiano S. Rodembusch,[d] João S. F. Guimarães,[f] André G. Oliveira,[f] Sebastian H. Röttger,[g] Daniel B. Werz,[g] Cauê P. Souza,[h] Felipe Fantuzzi,[h] Jianhua Han,[i] Todd B. Marder,[i] Holger Braunschweig*[i] and Eufrânio N. da Silva Júnior*[a]

[a]   Í. A. O. Bozzi, Dr. L. A. Machado, Msc. E. B. T. Diogo, Dr. F. G. Delolo, L. O. F. Barros, G. A. P. Graça, Prof. Dr. M. H. Araujo, Prof. Dr. E. N. da Silva Júnior
       Instituto de Ciências Exatas, Departamento de Química, Universidade Federal de Minas Gerais, Belo Horizonte, MG, 31270-901, Brazil
       E-mail: eufranio@ufmg.br
[b]   Prof. Dr. F. T. Martins
       Instituto de Química, Universidade Federal de Goiás, Goiânia 74690-900, Brazil
[c]   Prof. Dr. L. F. Pedrosa
       Departamento de Química, Universidade Federal Fluminense, 24020-141, RJ, Niterói, Brazil
[d]   L. C. da Luz, Prof. Dr. F. S. Rodembusch
       Instituto de Química, Universidade Federal do Rio Grande do Sul, Porto Alegre 91501-970 RS, Brazil
[e]   E. S. Moraes
       Universidade Estadual de Campinas (Unicamp), Cidade Universitária, 13083970 - Campinas, SP - Brazil
[f]   Dr. J. F. Guimarães, Prof. Dr. A. G. Oliveira
       Departamento de Fisiologia e Biofísica, Instituto de Ciências Biológicas, Universidade Federal de Minas Gerais, Belo Horizonte, Brazil
[g]   S. H. Röttger, Prof. Dr. D. B. Werz
       DFG Cluster of Excellence livMatS @FIT and Albert-Ludwigs-Universität Freiburg, Institute of Organic Chemistry, Albertstraße 21, 79104 Freiburg (Breisgau), Germany
[h]   C. P. Souza, Dr. F. Fantuzzi
       School of Chemistry and Forensic Science, University of Kent, Park Wood Rd, Canterbury CT2 7NH, United Kingdom
[i]   Dr. L. A. Machado, Dr. Jianhua Han, Prof. Dr. T. B. Marder, Prof. Dr. H. Braunschweig
       Institute for Inorganic Chemistry and Institute for Sustainable Chemistry & Catalysis with Boron, Julius-Maximilians-Universität Würzburg, Am Hubland, 97074 Würzburg, Germany
       E-mail: h.braunschweig@uni-wuerzburg.de
[+]   These authors contributed equally to this work.

       Supporting information for this article is given via a link at the end of the document.

Abstract: We report a rapid, efficient, and scope-extensive approach for the late-stage electrochemical diselenation of BODIPYs. Photophysical analyses reveal red-shifted absorption - corroborated by TD-DFT and DLPNO-STEOM-CCSD computations - and color-tunable emission with large Stokes shifts in the selenium-containing derivatives compared to their precursors. In addition, due to the presence of the heavy Se atoms, competitive ISC generates triplet states which sensitize $^1O_2$ and display phosphorescence in PMMA films at RT and in a frozen glass matrix at 77 K. Importantly, the selenium-containing BODIPYs demonstrate the ability to selectively stain lipid droplets, exhibiting distinct fluorescence in both green and red channels. This work highlights the potential of electrochemistry as an efficient method for synthesizing unique emission-tunable fluorophores with broad-ranging applications in bioimaging and related fields.

Introduction

BODIPYs are a well-known class of compounds that have high fluorescence quantum yields and good photostability, making them a popular choice for a wide range of applications.[1] Notably, they play a crucial role in fluorescence microscopy for bioimaging and are utilized to label proteins, nucleic acids, cell membranes, and other cellular structures, enabling detailed visualization and comprehensive analysis.[2] BODIPYs that exhibit red-shifted absorbance and photoluminescence in the red to near-infrared region of the spectrum, often referred to as the "biologically transparent window", have garnered significant attention. This attribute proves advantageous for biological and medical imaging applications as it allows for deeper tissue penetration (with less light absorption by the tissue) and reduced background autofluorescence when compared to dyes that absorb and emit in higher energy regions of the spectrum. However, most red-emitting BODIPYs demonstrate lower emission quantum yields compared to their blue-green-emitting counterparts, potentially constraining their effectiveness in specific contexts.[3,4] The emission properties of BODIPYs can be tailored by modifying the chromophore structure and introducing various functional groups.[5] Specifically, BODIPY derivatives decorated with chalcogens have been intensively studied to produce fluorescent probes for the detection of bioactive molecules.[6] The incorporation of chalcogens at positions 8 (*meso*),[7] and positions 3 and 5 (α) has been explored (Scheme 1A).[8] Additionally, the synthesis of fused rings involving position 1 and substituents at position 8 has also been reported.[9]

However, selenation at positions 2 and 6 has been scarcely explored. A study by Ortiz and colleagues revealed that heavy-atom substitution at the 2,6-positions has the most significant impact on intersystem crossing (ISC) quantum yields.[10] While various synthetic techniques are available for functionalizing BODIPYs, classical nucleophilic aromatic substitution (SNAr) methods cannot be employed to introduce heteroatom-containing

RESEARCH ARTICLE

substituents at the 2,6-positions due to the small coefficients in the LUMO at those positions. Functionalization at these positions typically relies on strategies such as electrophilic aromatic substitution (S$_E$Ar), Pd-catalyzed cross-coupling, and C–H activation reactions (Scheme 1B).[11] Klán and collaborators developed a two-step process for the preparation of mono- and disubstituted BODIPYs containing selenium at positions 2 and 6. The first step involves the displacement of hydrogen at these positions by halogen atoms using succinimide reagents such as NCS (Cl), NBS (Br), and NIS (I). Subsequently, with these halogens in place, post-functionalization is carried out using a Pd-catalyzed C–heteroatom Stille cross-coupling reaction.[12] Other Pd-catalyzed cross-couplings such as Suzuki-Miyaura and Sonogashira reactions can also be employed for this type of functionalization. Kubo[13] and Manjare[14] prepared a 2,6-diselenated BODIPY through S$_E$Ar using toxic phenylselanyl chloride as a reactant. Churchill and co-workers utilized both strategies to produce a selenium-containing BODIPY (Scheme 1C).[15] However, in all the cited examples, the methods employed necessitate prior functionalization, result in low yields of BODIPY derivatives or have limited reaction scope.

Electrocatalytic C–H activation has emerged as an exceptionally powerful tool for sustainable late-stage functionalization.[16a-d] Electrochemistry has also been useful for functionalizing heterocycles, including with the insertion of chalcogens, highlighting its potential to access molecules with broad applications in e.g., medicine and materials science.[16e-g] Recently, we have developed a rapid, green, and efficient protocol for the electrochemical selenation/cyclization of quinones to access bioactive compounds.[17] Herein, we present a sustainable and versatile electrochemical approach for 2,6-diselenation of BODIPYs using Pt(+)||C(-), reticulated vitreous carbon (RVC = C), as electrodes in undivided electrochemical cells. This innovative protocol bypasses the need for chemical oxidants and affords the swift synthesis of selenium-containing BODIPYs with good yields. The use of diselenides as reactants provides ease of handling, stability, odorlessness, and non-toxicity. To the best of our knowledge, this represents the first report showcasing the use of electrochemistry for late-stage diversification of BODIPYs (Scheme 1D).
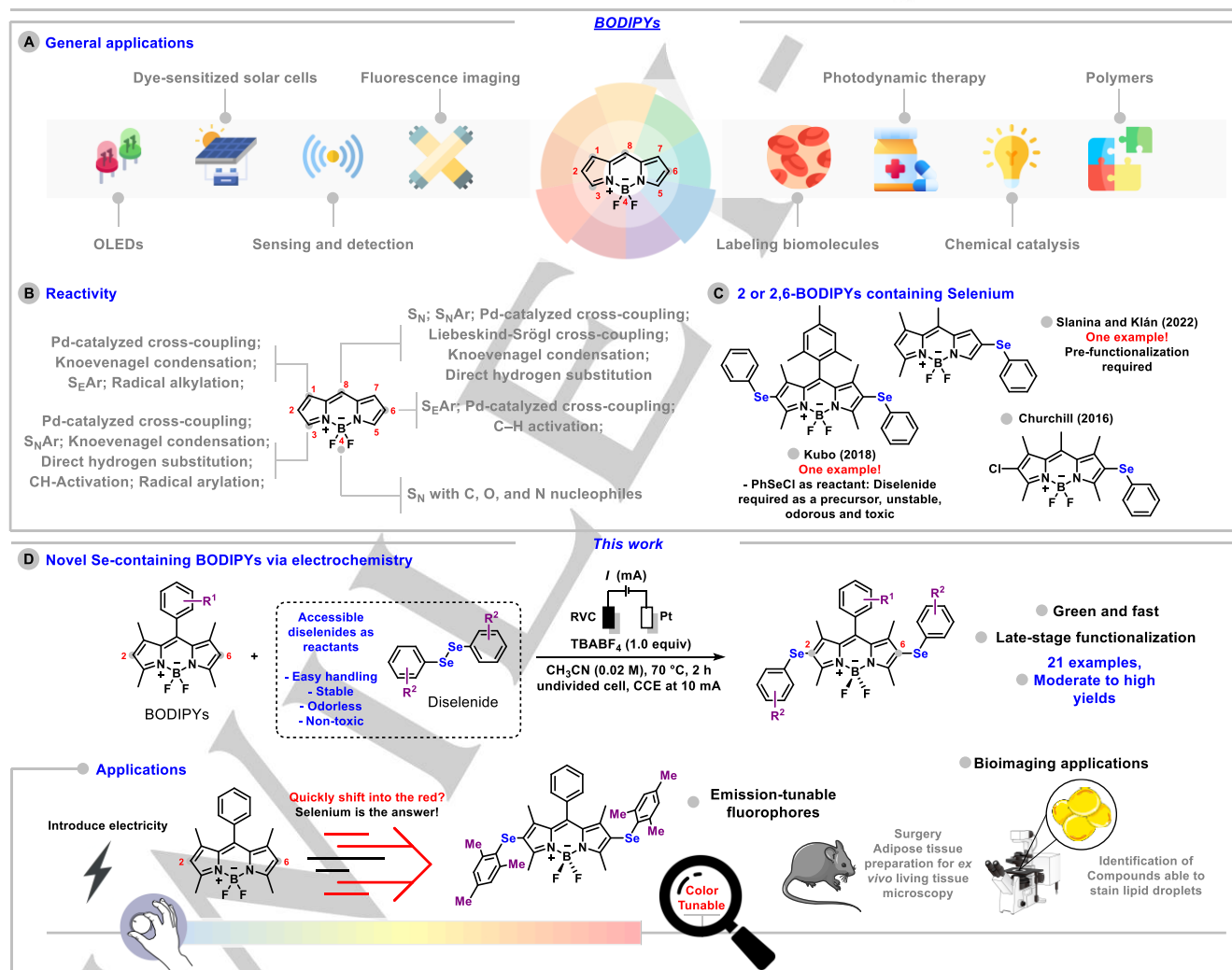
Scheme 1. Overview: A) Applications. B) Reactivity of BODIPYs. C) Examples of selenium-containing BODIPYs. D) Strategy for the synthesis of novel selenium-containing BODIPYs via electrochemistry.
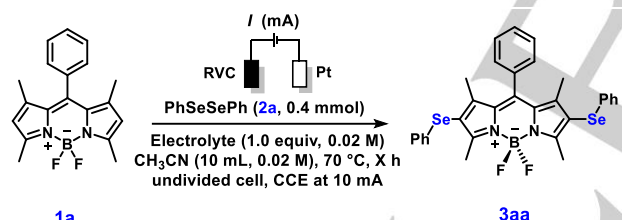
Results and Discussion

RESEARCH ARTICLE

We started our investigation on the electrochemical selenation using BODIPY **1a** and 1,2-diphenyldiselenide **2a** as substrate models. Using two undivided platinum electrodes (Pt(+)||Pt(-)) and TBAPF$_6$ as the electrolyte in MeCN solution, the product **3aa** was obtained in 42 or 52% yields within 1 or 2 h, respectively (Table 1, entries 1-2). By varying the electrode configuration (Table 1, entries 3-5), we observed that the combination of Pt(+)||RVC(-) favored the reaction, leading to a 67% yield of the desired product (Table 1, entry 5). Next, we evaluated different electrolytes (Table 1, entries 6-9) and found that the Pt(+)||RVC(-) system with TBABF$_4$ provided the best performance, resulting in a 71% isolated yield of the desired product (Table 1, entry 9). In the absence of an applied current, no reaction occurred (Table 1, entry 10).

We proceeded to investigate the substrate scope and limitations of the optimized process under the conditions described (Scheme 2). Initially, we examined the electrochemical selenation of BODIPYs with various substituents, including a thiophene moiety. Products **3ba**-**3ga**, which contained electron-donating groups (EDGs) such as alkyl or ether groups at the *para*-position of the phenyl ring, were obtained in yields ranging from 40 to 62%. Interestingly, selenium was successfully inserted at the desired position even in the presence of an alkyne group, resulting in product **3ha** in 60% yield. Products containing electron-withdrawing groups (EWGs), such as *p*-Cl (**3ia**), *p*-CN (**3ja**), and *p*-NO$_2$ (**3ka**), were obtained in moderate yields in the range of 25-35%. The product containing the *p*-SMe (**3la**) group was isolated in 40% yield, while the naphthyl derivative afforded **3ma** in 45% yield. The replacement of the phenyl group by thienyl (**3na**) significantly affected the performance of the reaction, resulting in a yield of 25%.

Table 1. Electrochemical 2,6-diselenation: Investigation of the reaction conditions using compounds **1a** and **2a** as substrates.[a]

Entry	Electrodes	Electrolytes	Current/mA	Time/h	Yield/%
1	Pt(+) || Pt(-)	TBAPF$_6$	20	1 h	42
2	Pt(+) || Pt(-)	TBAPF$_6$	20	2 h	52
3	RVC(+) || Pt(-)	TBAPF$_6$	20	2 h	36
4	RVC(+) || RVC(-)	TBAPF$_6$	20	2 h	56
5	Pt(+) || RVC(-)	TBAPF$_6$	20	2 h	67
6	Pt(+) || RVC(-)	KPF$_6$	20	2 h	57
7	Pt(+) || RVC(-)	TBAI	20	2 h	trace
8	Pt(+) || RVC(-)	TBABr	20	2 h	34
9	Pt(+) || RVC(-)	TBABF$_4$	10	2 h	71
10	Pt(+) || RVC(-)	TBABF$_4$	0	2 h	NR

[a] Reaction conditions: **1a** (0.2 mmol), **2a** (0.4 mmol, 2 equiv.), electrodes (10 mm × 10 mm × 0.05 mm), electrolyte (0.2 mmol, 1 equiv., 0.04 M), MeCN (10 mL, 0.04 M), current (0-20 mA), 70 °C, 1-2 h. RVC = Reticulated vitreous carbon. NR: no reaction.

The use of diphenylditelluride and diphenyldisulfide was also evaluated. The formation of the product **3oa** substituted with tellurium was not observed, even with variations of the method described here and reaction times of 2, 4, 8, and 16 h. On the other hand, the sulfur insertion reaction, under the electrochemical conditions established here, resulted in product

3pa with a 20% yield. We also considered BODIPYs with different substituent patterns and the use of an Aza-BODIPY derivative. In general, the method proved reliable for the insertion of selenium in disubstituted systems **3qa**, but did not allow the formation of the selenium-containing products **3ra** and **3sa**, when highly aryl-substituted systems were used. Selenium-containing BODIPYs were successfully obtained from a variety of aryl diselenides (Scheme 2). The trimethyl-substituted product (**3ab**) was obtained in 55% yield. Products with *o*-Me (**3ac**) and *o*-OMe (**3ad**) substituents were obtained at 70% and 40%, respectively. Products containing the EWGs *p*-Cl (**3ae**) and *p*-F (**3af**) were obtained in yields of 60% and 77%, respectively. The naphthylselenyl-substituted product containing **3ag** was obtained in 35% yield. A proposed mechanism and a discussion based on data from the literature can be found in the Supporting Information (SI, Scheme S1). The products were all purified and characterized by ^{1}H and ^{13}C NMR analysis as well as HRMS (see SI for details). The structure of **3ha** was also confirmed by X-ray crystallographic analysis and is presented in Scheme 2.

The photophysical characterization of the selenium-containing BODIPY derivatives was conducted in various organic solvents (10^{-5}-10^{-6} M) with different dielectric constants (1,4-dioxane, dichloromethane, ethanol, and acetonitrile). Detailed photophysical data for all precursors (**1a**-**1n**) and their respective derivatives (**3aa**-**3ng**) are summarized in Tables S1-S2. In dichloromethane, the selenium-containing BODIPYs exhibited absorption maxima between 515 and 545 nm, depending on the substituents (Figure 1). These absorptions are attributed to allowed $^1\pi$–π^* electronic transitions ($\varepsilon \sim 10^4$ M^{-1} cm^{-1}). Interestingly, diselenation led to a red-shift of the absorption maxima by ca. 20 nm compared to the respective precursors (Figures S4-S37). The Se-containing BODIPYs displayed color-tunable emission with maxima between 572-602 nm (Table 2, Figure 1). Upon selenation, the emission maxima shifted by ca. 70 nm to longer wavelengths compared to the respective precursors, indicating that the selenium atom plays a significant role in tuning the emission maxima of these compounds. In addition, no apparent pattern suggesting a significant charge transfer character in the ground and excited states are observed, consistent with preceding reports for other BODIPY derivatives.[1f,3d,3g] These compounds exhibited modest fluorescence quantum yields (~ 0.3%), as previously observed for selenium-based BODIPYs.[7c-7e,7i,8a,8c,9] This can still be useful for turn off-on sensing, as observed in several compounds,[18] and even in selenium-containing BODIPY-based ones.[19] Finally, the selenium derivatives exhibited significantly larger Stokes shifts (~2000 cm^{-1}) compared to the starting BODIPYs (~500 cm^{-1}), previously reported compounds (~400 cm^{-1}),[1f,3d,3g] and even BODIPY Lipid probes, that usually show a strong overlap between the fluorescence and absorption spectra,[20] resulting in a substantial reduction in the inner filter effect. The selenium-containing BODIPYs showed broad emission compared to reported BODIPYs, which could be used to enable imaging.[21a] In this case, the observed broad emission is likely associated with intrinsic vibronic coupling and structural relaxation of the S1 state, a phenomenon commonly observed in π-conjugated organic fluorophores.[21b] Similar trends were found for the other solvents studied (see SI). Furthermore, in nonpolar solvents such as hexane and toluene, these selenium derivatives demonstrate photophysical behavior remarkably similar to that observed in more polar solvents. This observation leads us to posit the

absence of the intramolecular charge transfer (ICT) process in these derivatives. It is noteworthy that the naphthyl derivative **3ag** exhibits dual fluorescence emission. Through analysis of the maxima locations in the studied solvents and taking their excitation spectra into account (see SI), the possibility of an ICT mechanism was ruled out. In this instance, the dual emission is anticipated to arise from two separate vibrational structures present in the excited state. The fluorescence lifetimes of the

precursors (~4 ns) are in accordance with what is expected for BODIPY derivatives.[3g] On the other hand, the selenium-based BODIPYs showed shorter fluorescence lifetimes, ranging from 2.24 to 0.32 ns, with an average lifetime of ca. 0.8 ns. The short lifetimes and modest quantum yields are consistent with competitive intersystem crossing (ISC) to the triplet state.
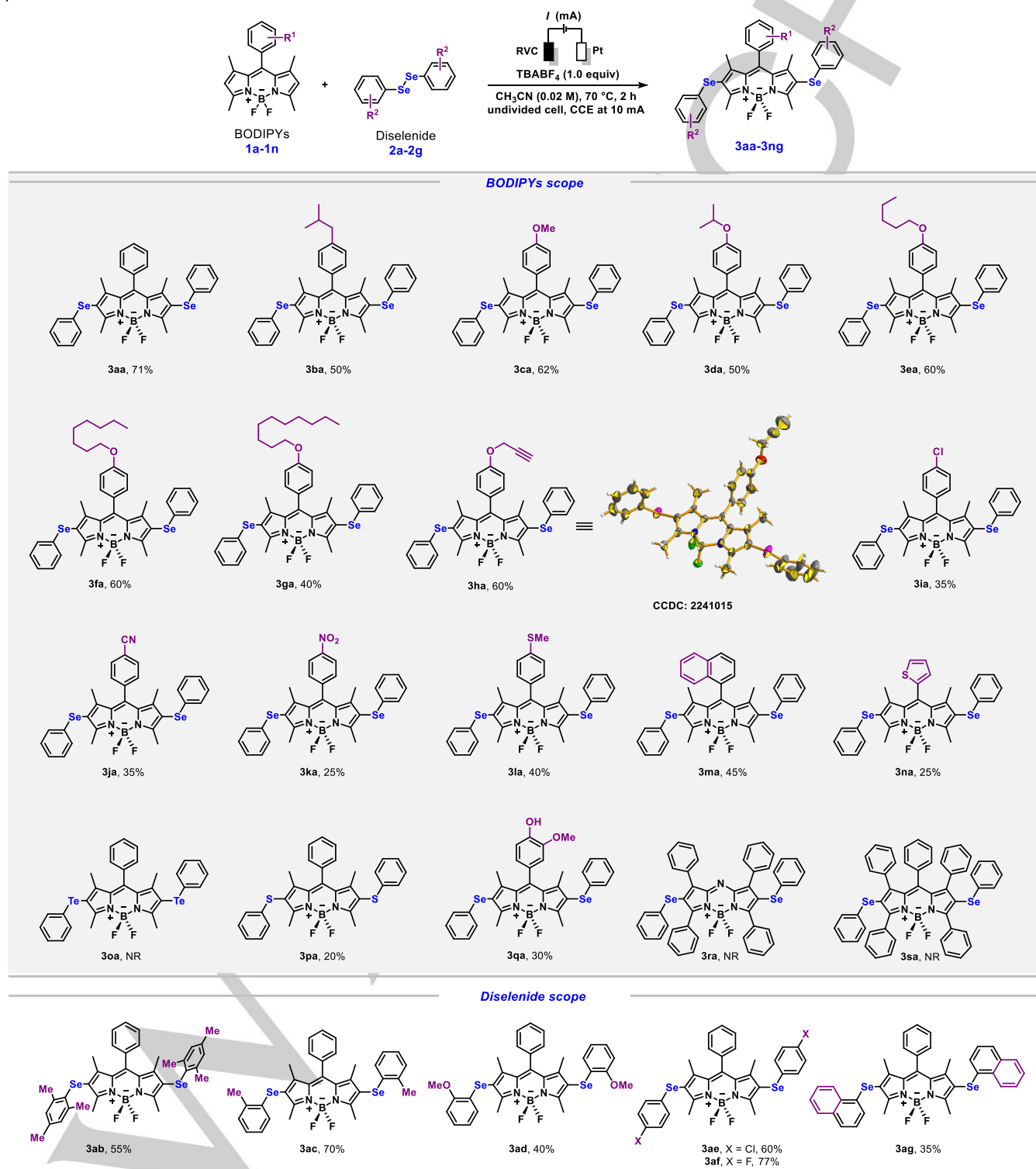

Scheme 2. Substrate scope: [a]BODIPY substrate (0.2 mmol), diselenide (0.4 mmol, 2 equiv.), MeCN (10 mL, 0.02 M), TBABF$_4$ (0.02 M, 1.0 equiv.), Pt(+) || RVC(-) (10 mm, 10 mm, 0.2 mm), undivided cell, current (10 mA), 70 °C, 2 h. NR = No reaction.

4

RESEARCH ARTICLE

Table 2. Photophysical data for selenium-containing BODIPYs **3aa-3ng** in dichloromethane, where λ_{abs} and λ_{em} are the absorption and emission maxima, respectively, ε is the molar absorptivity, and Φ_{FL} is the fluorescence quantum yield (%).

BODIPY	λ_{abs} (nm)	ε ($M^{-1} \cdot cm^{-1}$)	λ_{em} (nm)	Stokes shift (cm^{-1})	Φ_{FL}
3aa	515	69000	578	2120	0.35
3ba	515	81000	577	2090	0.34
3ca	515	95000	579	2150	0.30
3da	515	95000	577	2090	0.30
3ea	515	74000	577	2090	0.35
3fa	515	63000	577	2090	0.41
3ga	515	73000	577	2090	0.38
3ha	516	94000	578	2080	0.29
3ia	519	80000	580	2030	0.37
3ja	521	61000	589	2220	0.28
3ka	524	78000	595	2280	0.29
3la	518	65000	580	2060	0.37
3ma	521	73000	580	1950	0.35
3na	530	74000	595	2060	0.22
3pa	516	70000	580	2138	0.10
3qa	516	33000	580	2138	0.80
3ab	545	42000	602	1740	0.55
3ac	517	49000	579	2070	0.35
3ad	516	72000	580	2140	0.10
3ae	516	70000	576	2020	0.47
3af	515	67000	578	2120	0.37
3ag	518	72000	526/572	294/1820	0.29
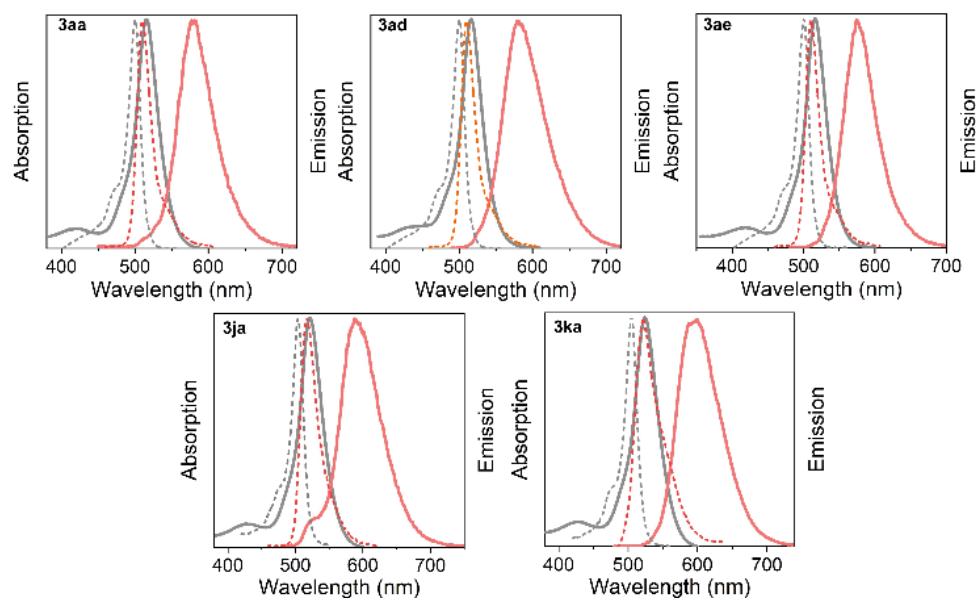
Figure 1. Normalized UV-Vis absorption spectra (in black) and steady-state fluorescence emission spectra (in red) in a dichloromethane solution [ca. 10^{-5} M] are shown for selected selenium-containing BODIPY derivatives: **3aa**, **3ad**, **3ae**, **3ja**, and **3ka**. Additionally, the respective precursors **1a** (for **3aa**, **3ad**, and **3ae**), **1j** (for **3ja**), and **1k** (for **3ka**) are presented for comparison, indicated by the respective dashed lines.

To investigate the photophysical properties of precursors and their derivatives for potential use in membrane/lipid staining, we conducted steady-state characterizations in a pH 7.0 PBS buffered solution (see SI for details). Notably, both sets of compounds exhibited broader absorption spectra in this aqueous environment compared to organic solvents. Precursors had absorption maxima around 500 nm, and the selenium-substituted

BODIPY dyes peaked at 520 nm, mirroring trends seen in organic solvents. Regarding their emission spectra, those of the precursors peaked at 510 nm with low QY values, while those of the derivatives showed even greater redshifts in comparison to organic solvents, with peaks around 580 nm.

Considering the modest quantum yields and short lifetimes, it seems that intersystem crossing (ISC) leading to triplet

5

RESEARCH ARTICLE

formation was a likely cause. Thus, the phosphorescent properties in solution and in PMMA films of selected derivatives were investigated (additional details and discussions, see SI). In general, the Se-BODIPYs exhibit, in addition to fluorescence, an additional red-shifted band located at ca. 740 nm with lifetimes between 200 ns and 1 ms. The Se-BODIPY dyes phosphoresce in PMMA film at room temperature and in a frozen glass matric at 77K, confirming the formation of a triplet state via ISC. That being the case, we then examined representative compounds **3ba**, and **3da-ga** for their ability to sensitize singlet oxygen ($^1O_2$), arising from their triplet states, which could potentially be applied in photoactivated selective killing of cells (i.e., photodynamic therapy). Indeed, as shown in Figure 2, all of the compounds examined generated $^1O_2$ when excited at 360 nm, as evidenced by the phosphorescent emission of $^1O_2$ at 1272 nm in the NIR. The quantum yields for $^1O_2$ formation (Φ_Δ) were in the range of 0.3-0.5. This also suggests very similar rate constants for fluorescence and ISC processes in the Se-containing BODIPYs.
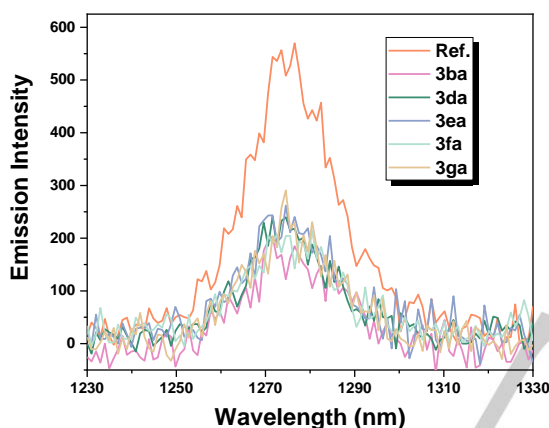

Figure 2. Emission spectrum of singlet oxygen generated from sensitization of a perinaphthenone standard (Ref.) vs. that generated by sensitization by compounds **3ba** ($\Phi_\Delta = 0.3$), **3da** ($\Phi_\Delta = 0.4$), **3ea** ($\Phi_\Delta = 0.5$), **3fa** ($\Phi_\Delta = 0.4$), **3ga** ($\Phi_\Delta = 0.4$), excited at 360 nm in dichloromethane.

To gain further insight into the electronic properties of these molecules, we conducted TD-DFT calculations on a selected set of compounds. The appropriate level of theory was determined via benchmarking against the X-ray crystal structure of **3ha** and experimental spectra (see SI for details). Geometry optimizations were carried out at the ωB97X-D/cc-pVDZ,aug-cc-pVTZ(Se) level in Gaussian 16. All geometries were confirmed as minima based on frequency calculations. TD-DFT (singlets) calculations were carried out on the optimized systems without the Tamm–Dancoff approximation but with the inclusion of the RIJCOSX approximation, performed at the ωB97X-D3(BJ)/def2-TZVP level. Solvation effects were considered through the implicit conductor-like polarizable continuum model (CPCM; solvent: dichloromethane, DCM) in ORCA 5.0.3. The character of the transitions was interpreted using natural transition orbital (NTO) analysis.

The significant absorption features observed in the visible region for all BODIPYs are attributed to the $S_0 \rightarrow S_1$ electronic transition (see SI for details). Although prior studies have underscored the disparities between calculated TD-DFT excitation energies and experimental data for BODIPYs,[22] TD-

DFT retains its significance as a valuable tool for evaluating electronic transition characteristics and qualitative patterns in absorption features within the BODIPY family. In our calculations, deviations fall within the range of 0.30 eV to 0.53 eV, with the propynyloxyphenyl-substituted molecules (**1h**, **3ha**) exhibiting a slightly more accurate representation compared to those featuring the simpler phenyl group (**1a**, **3aa**). Furthermore, better agreement is observed for the precursor compounds (**1a**, **1h**) when contrasted with the diselenide derivatives (**3aa**, **3ha**). All higher transitions occur within the UV spectral range and are not relevant to our discussion.

In light of the large excitation energy deviations observed with the TD-DFT method, we employed a more accurate approach to describe the excited states of these molecules better. Specifically, we turned to the coupled-cluster singles and doubles (CCSD) model, incorporating the similarity transformed equation of motion (STEOM) approach, and the domain-based local pair natural orbital (DLPNO) approximation formalism, denoted as DLPNO-STEOM-CCSD, and conducted these calculations using ORCA 5.0.3. These were done at the DFT optimized geometries and also applying the CPCM implicit solvent model (solvent: DCM). A benchmark of basis sets indicated that employing the double-ζ quality def2-SVP basis set sufficed (see SI for details).

As anticipated, this higher-level theoretical approach yielded a more accurate description of singlet excitation energies compared to TD-DFT (see Figure 3). The discrepancies ranged from 0.11 eV to 0.18 eV (see SI). Consistent with the TD-DFT results, a better agreement was observed for the precursor compounds compared to their diselenide derivatives. Furthermore, both TD-DFT ($\Delta\lambda = 10$ nm) and DLPNO-STEOM-CCSD ($\Delta\lambda = 34$ nm) calculations indicated a bathochromic shift when transitioning from precursor **1a** to its diselenide derivative **3aa**, aligning with experimental observations. Notably, the bathochromic effect aligns better with experimental data ($\Delta\lambda = 15$ nm) in the TD-DFT perspective. One possible explanation for this discrepancy might be the size-extensive nature of errors introduced by the DLPNO scheme,[23] which leads to more significant deviations in energy calculations for the derivatives compared to their respective precursors. This effect is not present in TD-DFT.

Despite the tendency of TD-DFT to overestimate transition energies, the bathochromic effect induced by diselenide substitution is qualitatively captured. As previously discussed, and supported by existing literature,[24] the $S_0 \rightarrow S_1$ transitions in BODIPYs are typically attributed to $^1\pi$–π^* transition characterized by minimal charge transfer, typical for HOMO-LUMO (H-L) transitions. The NTO analysis depicted in Figure 3 aligns with this picture. For all of the molecules, the electron densities of the relevant orbitals are predominantly localized over the three-fused-ring moieties, with a minor contribution in the 8-Ph substituent and the non-bonding electron pairs of the fluorides on the acceptor orbitals. Of particular interest to our investigation is the influence of the Se-containing substituents. As illustrated in Figure 3, Se atoms actively participate in both donor and acceptor orbitals. This leads to a more dispersed electron density in the Se-containing molecules when compared to the precursors, thereby narrowing their HOMO-LUMO gaps, an effect akin to what is observed with increased π-conjugation. Consequently, this reduction in the energy gap between the S_0 and S_1 states in the diselenated BODIPYs results in the observed bathochromic effect.
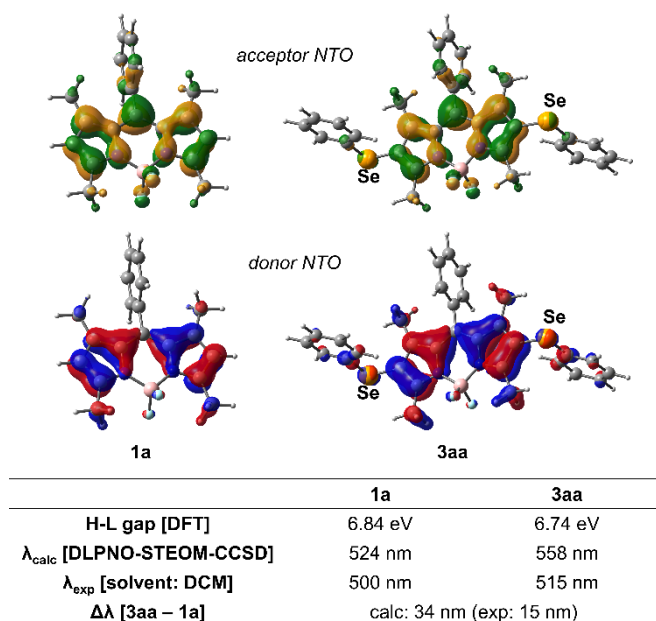
RESEARCH ARTICLE

	1a	3aa
H-L gap [DFT]	6.84 eV	6.74 eV
λ_{calc} [DLPNO-STEOM-CCSD]	524 nm	558 nm
λ_{exp} [solvent: DCM]	500 nm	515 nm
$\Delta\lambda$ [3aa − 1a]	calc: 34 nm (exp: 15 nm)	

Figure 3. Donor (hole) and acceptor (electron) NTO plots of **1a** and **3aa**. The DFT HOMO-LUMO (H-L) gap and the excitation energies (λ_{calc}: $S_0 \rightarrow S_1$ vertical excitation calculations at DLPNO-STEOM-CCSD; λ_{exp}: measured data) of the compounds in DCM are also shown. A bathochromic shift of $\Delta\lambda = 34$ nm is estimated by the computations, in good agreement with the experimental data ($\Delta\lambda = 15$ nm). Isovalues: 0.03 au.

Finally, we have demonstrated the potential of the selenium-containing BODIPYs for imaging of biological samples (Figure 4). Two pairs of non-selenated compounds and their corresponding selenated derivatives were selected for bioimaging studies, with living adipose tissue observed using a confocal microscope. The BODIPYs were excited at wavelengths of 488 nm and 535 nm. In the case of BODIPYs **1a** and **1h**, staining of lipid droplets was observed mostly in the green channel. In contrast, the selenium-

containing compounds **3aa** and **3ha** exhibited a consistent and significantly enhanced fluorescence in the red channel, in addition to their presence in the green channel, consistent with the broader emission spectra of these molecules. Importantly, the selected compounds stained structures that resembled the single large lipid droplet from adipocytes of unilocular white adipose tissue. This specificity was corroborated by comparing such a pattern with that observed following osmium tetroxide staining (see SI), a classical stain commonly used for the light and electron microscopy of adipose tissue.[25] These findings underscore the ability of these compounds to stain lipid droplets in different excitation/emission spectra, thereby demonstrating their potential as versatile fluorescent probes with broad-ranging applications. BODIPYs that absorb and emit at wavelengths ≥530nm can be detected in deeper layers of the tissues with decreased cytotoxicity.[26] Therefore, these probes can be employed to visualize various biological processes associated with lipid accumulation, both in living and fixed tissues, in physiological and pathological conditions such as fatty liver disease and obesity/metabolic syndrome.

Conclusion

In conclusion, we have successfully synthesized a diverse array of selenium-containing BODIPYs, using a rapid and efficient electrochemical method. The resulting selenium-containing BODIPYs exhibit useful and diverse photophysical features, including color-tunable emission associated with larger Stokes shifts than those of their precursors, and sensitization of $^1O_2$ from triplet states formed by competitive ISC, which makes them suitable for bioimaging studies and, potentially, for photodynamic therapy. Finally, this work demonstrates the potential of electrochemistry as a valuable approach for producing fluorescent probes with BODIPYs.
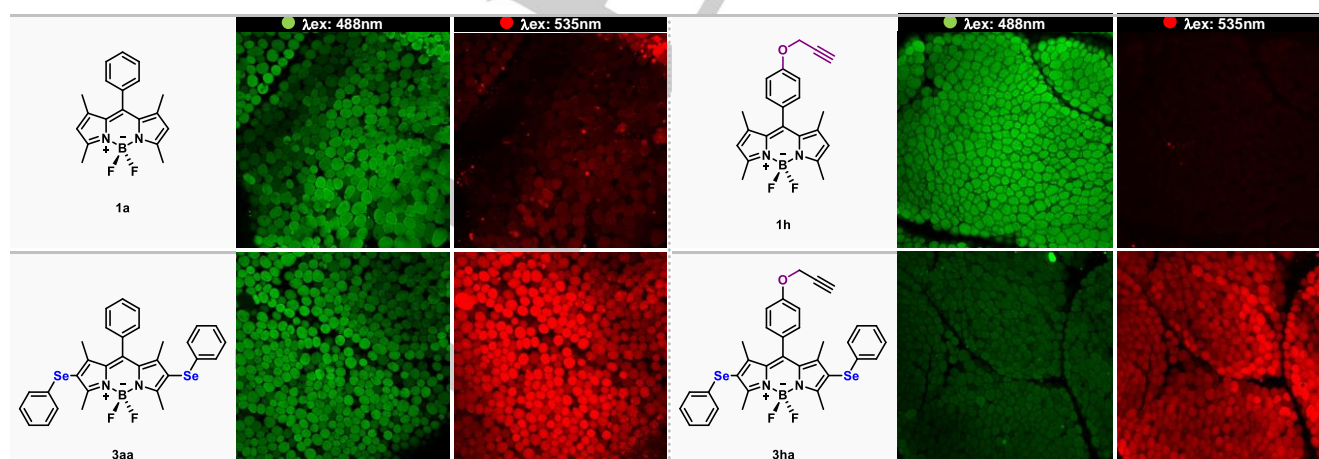

Figure 4. Bioimaging of lipid droplets in adipose tissue stained with non-selenated and selenated compounds. Tissues were excited at 488 nm or 535 nm and observed at 20x magnification. Scale: 120 μm.

Experimental Section

General procedure for the electrochemical diselenation of BODIPYs: In an electrochemical reactor, the corresponding BODIPY (0.2 mmol), TBABF$_4$ (0.2 mmol), and diselenide (0.4 mmol) were dissolved in 10 mL of MeCN. The reaction was

carried out at 70 °C using Pt(+)||RVC(-) under 10 mA and 20 V for 2 h. Then, the solvent was removed, and the product was purified by column chromatography using a hexane:toluene mixture as eluent.

Author contributions

7

WILEY-VCH

RESEARCH ARTICLE

Conflict of interest

I.A.O.B., F.G.D., F.S.R., A.G.O., and E.N.S.J. are inventors on a pending patent related to the technology described in this work.

Supporting Information

All synthetic procedures, analytical data, photophysical studies, phosphorescence measurements, cyclic voltammetry, crystallographic, bioimaging and computational data are available in the supplementary material of this article. Cambridge Crystallographic Data information on the structure **3ha**.[27] The authors have cited additional references within the Supporting Information.[28-63]

Acknowledgments

Keywords: BODIPY • selenium • electrochemistry • NIR • fluorophores

[1] (a) N. Boens, V. Leen, W. Dehaen, *Chem. Soc. Rev.* **2012**, *41*, 1130–1172; (b) A. Loudet, K. Burgess, *Chem. Rev.* **2007**, *107*, 11, 4891–4932; (c) A. Kamkaew, S. H. Lim, H. B. Lee, L. V. Kiew, L. Y. Chung, K. Burgess, *Chem. Soc. Rev.* **2013**, *42*, 77–88; (d) A. Turksoy, D. Yildiz, E. U. Akkaya, *Coord. Chem. Rev.* **2019**, *379*, 47–64; (e) P. Lu, K.-Y. Chung, A. Stafford, M. Kiker, K. Kafle, Z. A. Page, *Polym. Chem.* **2021**, *12*, 327–348; (f) J. Patalag, S. Ahadi, O. Lashchuk, P. G. Jones, S. Ebbinghaus, D. B. Werz,

Angew. Chem. Int. Ed. **2021**, *60*, 8766–8771; *Angew. Chem.* **2021**, *133*, 8848–8853.

[2] (a) P. Kaur, K. Singh, *J. Mater. Chem. C* **2019**, *7*, 11361–11405; (b) A. C. Scanone, S. C. Santamarina, D. A. Heredia, E. N. Durantini, A. M. Durantini, *ACS Appl. Bio Mat.* **2020**, 3, 1061–1070; (c) B. Sui, S. Tang, T. Liu, B. Kim, K. D. Belfield, *ACS Appl. Mater. Interfaces* **2014**, *6*, 18408–18412; (d) W. Li, L. Wang, C. Zhang, X. Ran, H. Tang, D. Cao, *J. Mater. Chem. C* **2022**, *10*, 5672–5683; (e) H. T. Bui, D. K. Mai, B. Kim, K.-H. Choi, B. J. Park, H.-J. Kim, S. Cho, *J. Phys. Chem. B* **2019**, *123*, 26, 5601–5607; (f) T. Zhang, C. Ma, T. Sun, Z. Xie, *Coord. Chem. Rev.* **2019**, *390*, 76–85.

[3] (a) L. Yuan, W. Lin, K. Zheng, L. He, W. Huang, *Chem. Soc. Rev.* **2013**, *42*, 622–661; (b) Y. Ni, J. Wu, *Org. Biomol. Chem.* **2014**, *12*, 3774–3791; (c) Y. Zhang, K.-H. Song, S. Tang, L. Ravelo, J. Cusido, C. Sun, H. F. Zhang, F. M. Raymo, *J. Am. Chem. Soc.* **2018**, *140*, 12741–12745; (d) L. J. Patalag, P. G. Jones, D. B. Werz, *Angew. Chem. Int. Ed.* **2016**, *55*, 13340–13344; *Angew. Chem.* **2016**, *128*, 13534–13539; (e) L. Sansalone, S. Tang, J. Garcia-Amorós, Y. Zhang, S. Nonell, J. D. Baker, B. Captain, F. M. Raymo, *ACS Sensors* **2018**, *3*, 1347–1353; (f) S. Jia, E. M. Sletten, *ACS Chem. Bio.* **2022**, *17*, 3255–3269; (g) A. Patra, L. J. Patalag, P. G. Jones, D. B. Werz, *Angew. Chem. Int. Ed.* **2021**, *60*, 747–752; *Angew. Chem.* **2021**, *133*, 758–763.

[4] The molecular probes® handbook: A guide to fluorescent probes and labelling technologies, Invitrogen Corporation, 11th Edition, 2010.

[5] (a) J. Bañuelos, *Chem. Rec.* **2016**, *16*, 335–348; (b) R. Zagami, G. Sortino, E. Caruso, M. C. Malacarne, S. Banfi, S. Patanè, L. Monsù Scolaro, A. Mazzaglia, *Langmuir* **2018**, *34*, 8639–8651; (c) A. Prieto-Castañeda, E. Avellanal-Zaballa, L. Gartzia-Rivero, L. Cerdán, A. R. Agarrabeitia, I. García-Moreno, J. Bañuelos, M. J. Ortiz, *ChemPhotoChem* **2019**, *3*, 75–85; (d) L. Bonardi, G. Ulrich, R. Ziessel, *Org. Lett.* **2008**, *10*, 2183–2186.

[6] (a) R. Mamgain, F. V. Singh, *ACS Org. Inorg. Au* **2022**, *2*, 262–288; (b) A. Abdillah, P. M. Sonawane, D. Kim, D. Mametov, S. Shimodaira, Y. Park, D. G. Churchill, *Molecules* **2021**, *26*, 692; (c) S. Panda, A. Panda, S. S. Zade, *Coord. Chem. Rev.* **2015**, *300*, 86–100; (d) J. Fernández-Lodeiro, M. F. Pinatto-Botelho, A. A. Soares-Paulino, A. C. Gonçalves, B. A. Sousa, C. Princival, A. A. Dos Santos, *Dyes Pigm.* **2014**, *110*, 28–48; (e) S. T. Manjare, Y. Kim, D. G. Churchill, *Acc. Chem. Res.* **2014**, *47*, 2985–2998.

[7] (a) K. Kim, C. Jo, S. Easwaramoorthi, J. Sung, D. H. Kim, D. G. Churchill, *Inorg. Chem.* **2010**, *49*, 4881-4894; (b) X. Lu, N. Wang, Y. Tao, J. Wang, X. Ji, J. Liu, W. Zhao, J. Zhang, *Chem. Commun.* **2022**, *58*, 12576–12579; (c) Y. Mei, H. Li, C.-Z. Song, X.-G. Chen, Q.-H. Song, *Chem. Commun.* **2021**, *57*, 10198–10201; (d) K. S. Madibone, P. P. Deshmukh, A. Navalkar, S. K. Maji, P. M. Badani, S. T. Manjare, *ACS Omega* **2020**, *5*, 23, 14186–14193; (e) P. P. Deshmukh, A. Navalkar, S. K. Maji, S. T. Manjare, *Sens. Actuators B: Chem.* **2019**, *281*, 8–13; (f) Y. Kim, T. Jun, S. V. Mulay, S. T. Manjare, J. Kwak, Y. Leed, D. G. Churchill, *Dalton Trans.* **2017**, *46*, 4111–4117; (g) D. P. Murale, S. T. Manjare, Y.-S. Lee, D. G. Churchill, *Chem. Commun.* **2014**, *50*, 359–361; (h) S. T. Manjare, S. Kim, W. D. Heo, D. G. Churchill, *Org. Lett.* **2014**, *16*, 410–412; (i) B. Wang, P. Li, F. Yu, P. Song, X. Sun, S. Yang, Z. Lou, K. Han, *Chem. Commun.* **2013**, *49*, 1014–1016.

[8] (a) G. S. Malankar, D. S. Shelar, M. Manikandan, M. Patra, S. T. Manjare, *J. Mol. Struct.* **2023**, *1281*, 135118; (b) Q. Wu, J. Yuan, C. Yu, Y. Wei, X. Mu, L. Jiao, E. Hao, *J. Porphyr. Phthalocyanines* **2018**, *22*, 838–846; (c) B. Wang, F. Yu, P. Li, X. Sun, K. Han, *Dyes Pigm.* **2013**, *96*, 383–390; (d) B. Wang, P. Li, F. Yu, J. Chen, Z. Qu, K. Han, *Chem. Commun.* **2013**, *49*, 5790–5792; (e) E. Fron, E. Coutiño-Gonzalez, L. Pandey, M. Sliwa, M. Van der Auweraer, F. C. De Schryver, J. Thomas, Z. Dong, V. Leen, M. Smet, W. Dehaen, T. Vosch, *New J. Chem.* **2009**, *33*, 1490–1496.

[9] S. T. Manjare, J. Kim, Y. Lee, D. G. Churchill, *Org. Lett.* **2014**, *16*, 2, 520–523.

[10] M. J. Ortiz, A. R. Agarrabeitia, G. Duran-Sampedro, J. B. Prieto, T. A. Lopez, W. A. Massad, H. A. Montejano, N. A. Garcia, I. L. Arbeloa, *Tetrahedron* **2012**, *68*, 1153–1162.

[11] (a) E. Bodio, C. Goze, *Dyes Pigm.* **2019**, *160*, 700–710; (b) N. Boens, B. Verbelen, M. J. Ortiz, L. Jiao, W. Dehaen, *Coord. Chem. Rev.* **2019**, *399*, 213024; (c) V. Leen, D. Miscoria, S. Yin, A. Filarowski, J. M. Ngongo, M.

WILEY-VCH

RESEARCH ARTICLE

Van der Auweraer, N. Boens, W. Dehaen, *J. Org. Chem.* **2011**, *76*, 8168–8176; (d) N. Boens, B. Verbelen, W. Dehaen, *Eur. J. Org. Chem.* **2015**, 6577–6595.

[12] (a) M. Poljak, L. Wohlrábová, E. Palao, J. Nociarová, J. Míšek, T. Slanina, P. Klán, *Chem. Commun.* **2022**, *58*, 6389–6392; (b) E. Palao, T. Slanina, P. Klán, *Chem. Commun.* **2016**, *52*, 11951–11954.

[13] M. Nakashima, K. Iizuka, M. Karasawa, K. Ishii, Y. Kubo, *J. Mater. Chem. C* **2018**, *6*, 6208–6215.

[14] G. S. Malankar, A. Sakunthala, A. Navalkar, S. K. Maji, S. Raju, S. T. Manjare, *Anal. Chim. Acta* **2021**, *1150*, 338205.

[15] (a) S. V. Mulay, T. Yudhistira, M. Choi, Y. Kim, J. Kim, Y. J. Jang, S. Jon, D. G. Churchill, *Chem. Asian J.* **2016**, *11*, 3598–3605; (b) S. V. Mulay, M. Choi, Y. J. Jang, Y. Kim, S. Jon, D. G. Churchill, *Chem. Eur. J.* **2016**, *22*, 9642–9648.

[16] (a) L. Zhang, T. Ritter, *J. Am. Chem. Soc.* **2022**, *144*, 2399–2414; (b) N. Sauermann, T. H. Meyer, Y. Qiu, L. Ackermann, *ACS Catal.* **2018**, *8*, 7086–7103; (c) U. Dhawa, N. Kaplaneris, L. Ackermann, *Org. Chem. Front.* **2021**, *8*, 4886–4913; (d) C. Ma, P. Fang, T. -S. Mei, *ACS Catal.* **2018**, *8*, 7179–7189; (e) M. R. Scheide, C. R. Nicoleti, G. M. Martins, A. L. Braga, *Org. Biomol. Chem.* **2021**, *19*, 2578–2602; (f) M. R. Scheide, A. R. Schneider, G. A. M. Jardim, G. M. Martins, D. C. Durigon, S. Saba, J. Rafique, A. L. Braga, *Org. Biomol. Chem.* **2020**, *18*, 4916–4921; (g) G. M. Martins, A. G. Meirinho, N. Ahmed, A. L. Braga, S. R. Mendes, *ChemElectroChem* **2019**, *6*, 5928–5940.

[17] A. Kharma, C. Jacob, Í. A. O. Bozzi, G. A. M. Jardim, A. L. Braga, K. Salomão, C. C. Gatto, M. F. S. Silva, C. Pessoa, M. Stangier, L. Ackermann, E. N. da Silva Júnior, *Eur. J. Org. Chem.* **2020**, 4474–4486.

[18] B. T. Huy, D. T. Thangadurai, M. Sharipov, N. N. Nghia, N. V. Cuong, Y. I. Lee, *Microchem. J.* **2022**, *179*, 107511; (b) K. J. Bruemmer, S. W. M. Crossley, C. J. Chang, *Angew. Chem. Int. Ed.* **2020**, *59*, 13734–13762; *Angew. Chem.* **2020**, *132*, 13838–13867.

[19] S. T. Salunke, D. S. Shelar, S. T. Manjare, *J. Fluoresc.* **2023**, *33*, 437–444.

[20] (a) J. Karolin, L. B. A. Johansson, L. Strandberg, T. Ny, *J. Am. Chem. Soc.* **1994**, *116*, 7801–7806; (b) I. D. Johnson, H. C. Kang, R. P. Haugland, *Anal. Biochem.* **1991**, 198, 228–237.

[21] (a) P. Rodríguez-Sevilla, S. A. Thompson, D. Jaque, *Adv. NanoBiomed Res.* **2022**, *2*, 2100084; (b) J. M. Ha, S. H. Hur, A. Pathak, J. E. Jeong, H. Y. Woo, *NPG Asia Mater* 13, **2021**, 53.

[22] B. Le Guennic, D. Jacquemin, *Acc. Chem. Res.* **2015**, *48*, 530–537.

[23] I. Sandler, J. Chen, M. Taylor, S. Sharma, J. Ho, *J. Phys. Chem. A* **2021**, *125*, 1553–1563.

[24] E. Akhuseyin Yildiz, E. Yabaş, F. Sözmen, Y. Bozkurt, A. Karatay, B. Boyacioglu, H. Ünver, A. Elmali, *ChemPhysChem* **2023**, *24*, e202200735.

[25] (a) D. Belazi, S. Solé-Domènech, B. Johansson, M. Schalling, P. Sjövall, *Histochem. Cell. Biol.* **2009**, *132*, 105–115; (b) V. B. Wigglesworth, *Biol. Rev. Camb. Philos. Soc.* **1988**, *63*, 417–431.

[26] E. Antina, N. Bumagina, Y. Marfin, G. Guseva, L. Nikitina, D. Sbytov, F. Telegin, *Molecules* **2022**, *27*, 1396.

[27] Deposition Number(s) <url href="https://www.ccdc.cam.ac.uk/services/structures?id=doi:10.1002/chem.202303883X"> 2241015 (for **3ha**) </url> contain(s) the supplementary crystallographic data for this paper. These data are provided free of charge by the joint Cambridge Crystallographic Data Centre and Fachinformationszentrum Karlsruhe <url href="http://www.ccdc.cam.ac.uk/structures">Access Structures service</url>.

[28] C. Würth, M. Grabolle, J. Pauli, M. Spieles, U. Resch-Genger. *Nat. Protoc.* **2013**, *8*, 1535–1550.

[29] a) N. C. de Lucas, R. J. Corrêa, S. J. Garden, G. Santos, R. Rodrigues, C. E. M. Carvalho, S. B. Ferreira, J. C. Netto-Ferreira, V. F. Ferreira, P. Miro, M. L. Marin, M. A. Miranda, *Photochem. Photobiol. Sci.* **2012**, *11*, 1201-1209; b) J. Merz, L. Dietrich, J. Nitsch, I. Krummenacher, H. Braunschweig, M. Moos, D. Mims, C. Lambert, T. B. Marder, Chem. Sci. **2019**, 10, 7516-7534; c) M. Ferger, C. Roger, E. Köster, F. Rauch, S. Lorenzen, I. Krummenacher, A. Friedrich, M. Košćak, D. Nestić, H. Braunschweig, C. Lambert, I. Piantanida, T. B. Marder, *Chem. Eur. J.* **2022**, *28*, e202201130.

[30] a) A. Kunai, J. Harada, J. Izumi, H. Tachihara, K. Sasaki, *Electrochim. Acta* **1983**, *28*, 1361–1366; (b) J. Ludvík, B. Nygard, *J. Electroanal. Chem.* **1997**, *423*, 1–11; c) G. I. Giles, K. M. Tasker, R. J. K. Johnson, C. Jacob, C. Peers, K. N. Green, *Chem. Commun.* **2001**, 2490–2491; d) O. Niyomura, M. Cox, T. Wirth, Synlett 2006, 2, 251–254; e) B. Mueller, H. Poleschner, K. Seppelt, *Dalton Trans.* **2008**, 4424–4427; f) G. I. Giles, N. M. Giles, C. A. Collins, K. Holt, F. H. Fry, P. A. S. Lowden, N. J. Gutowski, C. Jacob, *Chem. Commun.* **2013**, *49*, 2030–2031; g) C. D. Prasad, S. J. Balkrishna, A. Kumar, B. S. Bhakuni, K. Shrimali, S. Biswas, S. Kumar, *J. Org. Chem.* **2013**, *78*, 1434–1443; h) S. Kumar, R. Kadu, S. Kumar, *Org. Biomol. Chem.* **2016**, *14*, 9210–9214; i) G. I. Giles, M. J. Nasim, W. Ali, C. Jacob, *Antioxidants* **2017**, *6*, 38; j) C. D. Prasad, M. Sattar, S. Kumar, *Org. Lett.* **2017**, *19*, 774–777; k) M. Wilken, S. Ortgies, A. Breder, I. Siewert, *ACS Catal.* **2018**, *8*, 10901–10912; l) L. Sun, Y. Yuan, M. Yao, H. Wang, D. Wang, M. Gao, Y.-H. Chen, A. Lei, *Org. Lett.* **2019**, *21*, 1297–1300; m) V. J. Richards, A. L. Gower, J. E. H. B. Smith, E. S. Davies, D. Lahaye, A. G. Slater, W. Lewis, A. J. Blake, N. R. Champness, D. L. Kays, *Chem. Commun.* **2012**, 48, 1751-1753; n) A. B. Nepomnyashchii, A. J. Bard, *Acc. Chem. Res.* **2012**, *45*, 1844–1853.

[31] W. Wu, H. Guo, W. Wu, S. Ji, J. Zhao, *J. Org. Chem.*, 2011, *76*, 7056–7064

[32] (a) L. J. Patalag, J. Hoche, R. Mitric, D. B. Werz, B. L. Feringa, *Angew. Chem. Int. Ed.*, **2022**, *61*, e202116834; *Angew. Chem.* **2022**, *134*, e2021168; (b) L. J. Patalag, L. P. Ho, P. G. Jones, D. B. Werz, *J. Am. Chem. Soc.*, **2017**, *139*, 15104–15113.

[33] J. Kang, F. Huo, P. Ning, X. Meng, J. Chao, C. Yin, *Sens. Actuators* B: *Chem.*, **2017**, *250*, 342-350.

[34] H.-B. Sun, S.-J. Liu, T.-C. Ma, N.-N. Song, Q. Zhao, W. Huang, *New J. Chem.*, **2011**, *35*, 1194-1197.

[35] B. Kilic, N. Yesilgul, V. Polat, Z. Gercek, E. U. Akkaya, *Tetrahedron Lett.*, **2016**, *57*, 1317-1320.

[36] C. Zhang, J. Zhao, S. Wu, Z. Wang, W. Wu, J. Ma, S. Guo, L. Huang, *J. Am. Chem. Soc.*, **2013**, *135*, 10566–10578.

[37] X. Zheng, L. Zhang, M. Ju, L. Liu, C. Ma, Y. Huang, B. Wang, W. Ding, X. Luan, B. Shen, *ACS Appl. Mater. Interfaces*, **2022**, *14*, 46262–46272.

[38] W. Ma, J. Du, J. Yin, J. Fan, S. Long, X. Peng, *Sens. Actuators B: Chem.*, **2018**, *267*, 104-110.

[39] H. Imahori, H. Norieda, H. Yamada, Y. Nishimura, I. Yamazaki, Y. Sakata, S. Fukuzumi, *J. Am. Chem. Soc.*, **2001**, *123*, 100–110.

[40] R. G. Almeida, R. L. de Carvalho, M. P. Nunes, R. S. Gomes, L. F. Pedrosa, C. A. de Simone, E. Gopi, V. Geertsen, E. Gravel, E., E. N. da Silva Júnior, *Catal. Sci. Technol.*, **2019**, *9*, 2742-2748.

[41] C. Li, T. Sun, Z. Li, Z. Xie, *ACS Appl. Nano Mater.*, **2022**, *5*, 18691-18696.

[42] J. H. Gibbs, L. T. Robins, Z. Zhou, P. Bobadova-Parvanova, M. Cottam, G. T. McCandless, F. R. Fronczek, M. G. H. Vicente, *Bioorg. Med. Chem.*, **2013**, *21*, 5770-5781.

[43] M. T. Páez González, S. M. G.Mello, F. S. Emery, *J. Fluoresc.* **2019**, *29*, 845–852

[44] APEX3, SAINT and SADABS. Bruker AXS Inc., Madison, Wisconsin, USA, **2015**.

[45] G. M. Sheldrick, *Acta Crystallogr. Sect. C*, **2015**, *71*, 3–8.

[46] L. J. Farrugia, *J. Appl. Crystallogr.*, **2012**, *45*, 849–854.

[47] a) C. R. Groom, I. J. Bruno, M. P. Lightfoot, S. C. Ward, *Acta Cryst.* **2016**, *B72*, 171-179; b) I. J. Bruno, J. C. Cole, M. Kessler, Jie Luo, W. D. S. Motherwell, L. H. Purkis, B. R. Smith, R. Taylor, R. I. Cooper, S. E. Harris, A. G. Orpen, *J. Chem. Inf. Comput. Sci.*, **2004**, *44*, 2133-2144; (c) S. J. Cottrell, T. S. G. Olsson, R. Taylor, J. C. Cole, J. W. Liebeschuetz, *J. Chem. Inf. Model.*, **2012**, *52*, 956-962.

[48] X.-F. Zhang, X. Yang, K. Niu, H. Geng, *J. Photochem. Photobiol. A* **2014**, *285*, 16-20.

[49] Z. Xiong, W. Gong, P. Xu, M. Jiang, X. Cai, Y. Zhu, X. Ping, H. Feng, H. Ma, Z. Qian, *Chem. Eng. J.* **2023**, *451*, 139030.

[50] a) T. H. Dunning, *J. Chem. Phys.* **1989**, *90*, 1007–1023; b) R. A. Kendall, T. H. Dunning, R. J. Harrison, *J. Chem. Phys.* **1992**, *96*, 6796–6806; c) D. E. Woon, T. H. Dunning, *J. Chem. Phys.* **1993**, *98*, 1358–1371; d) K. A. Peterson, D. E. Woon, T. H. Dunning, *J. Chem. Phys.* **1994**, *100*, 7410–7415; e) A. K. Wilson, D. E. Woon, K. A. Peterson, T. H. Dunning, *J. Chem. Phys.* **1999**, *110*, 7667–7676.

RESEARCH ARTICLE

[51] a) J.-D. Chai, M. Head-Gordon, *J. Chem. Phys.* **2008**, *128*, 084106; b) J.-D. Chai, M. Head-Gordon, *Phys. Chem. Chem. Phys.* **2008**, *10*, 6615; c) J.-D. Chai, M. Head-Gordon, *J. Chem. Phys.* **2009**, *131*, 174105.

[52] M. J. Frisch, G. W. Trucks, H. B. Schlegel, G. E. Scuseria, M. A. Robb, J. R. Cheeseman, G. Scalmani, V. Barone, G. A. Petersson, H. Nakatsuji, X. Li, M. Caricato, A. V Marenich, J. Bloino, B. G. Janesko, R. Gomperts, B. Mennucci, H. P. Hratchian, J. V Ortiz, A. F. Izmaylov, J. L. Sonnenberg, D. Williams-Young, F. Ding, F. Lipparini, F. Egidi, J. Goings, B. Peng, A. Petrone, T. Henderson, D. Ranasinghe, V. G. Zakrzewski, J. Gao, N. Rega, G. Zheng, W. Liang, M. Hada, M. Ehara, K. Toyota, R. Fukuda, J. Hasegawa, M. Ishida, T. Nakajima, Y. Honda, O. Kitao, H. Nakai, T. Vreven, K. Throssell, J. A. Montgomery Jr., J. E. Peralta, F. Ogliaro, M. J. Bearpark, J. J. Heyd, E. N. Brothers, K. N. Kudin, V. N. Staroverov, T. A. Keith, R. Kobayashi, J. Normand, K. Raghavachari, A. P. Rendell, J. C. Burant, S. S. Iyengar, J. Tomasi, M. Cossi, J. M. Millam, M. Klene, C. Adamo, R. Cammi, J. W. Ochterski, R. L. Martin, K. Morokuma, O. Farkas, J. B. Foresman, D. J. Fox, Gausian 16, Revision A.03, **2016**.

[53] a) F. Weigend, R. Ahlrichs, *Phys. Chem. Chem. Phys.* **2005**, *7*, 3297–3305; b) F. Weigend, *Phys. Chem. Chem. Phys.* **2006**, *8*, 1057–1065.

[54] a) F. Furche, R. Ahlrichs, *J. Chem. Phys.* **2002**, *117*, 7433–7447; b) R. Bauernschmitt, M. Häser, O. Treutler, R. Ahlrichs, *Chem. Phys. Lett.* **1997**, *264*, 573–578.

[55] a) S. Grimme, J. Antony, S. Ehrlich, H. Krieg, *J. Chem. Phys.* **2010**, *132*, 154104; b) S. Grimme, S. Ehrlich, L. Goerigk, *J. Comput. Chem.* **2011**, *32*, 1456–1465.

[56] D. M. York, M. Karplus, *J. Phys. Chem. A* **1999**, *103*, 11060–11079.

[57] a) F. Neese, *Wiley Interdiscip. Rev. Comput. Mol. Sci.* **2012**, *2*, 73–78; b) F. Neese, F. Wennmohs, U. Becker, C. Riplinger, *J. Chem. Phys.* **2020**, *152*, 224108; c) d) S. Lehtola, C. Steigemann, M. J. T. Oliveira, M. A. L. Marques, *SoftwareX* **2018**, *7*, 1–5. e) E. F. Valeev, "Libint: high-performance library for computing Gaussian integrals in quantum mechanics", can be found under https://github.com/evaleev/libint, **2021** (accessed 24 May 2023); f) F. Neese, *Wiley Interdiscip. Rev. Comput. Mol. Sci.* **2022**, *12*, e1606.

[58] a) R. L. Martin, *J. Chem. Phys.* **2003**, *118*, 4775–4777; b) E. R. Batista, R. L. Martin, in *Encyclopedia of Computational Chemistry*, John Wiley & Sons, Ltd, Chichester, UK, **2004**; c) F. Plasser, H. Lischka, *J. Chem. Theory Comput.* **2012**, *8*, 2777–2789; d) F. Plasser, M. Wormit, A. Dreuw, *J. Chem. Phys.* **2014**, *141*, 024106; e) F. Plasser, S. A. Bäppler, M. Wormit, A. Dreuw, *J. Chem. Phys.* **2014**, *141*, 024107.

[59] F. Plasser, *J. Chem. Phys.* **2020**, *152*, 084108.

[60] a) S. H. Vosko, L. Wilk, M. Nusair, *Can. J. Phys.* **1980**, *58*, 1200–1211; b) C. Lee, W. Yang, R. G. Parr, *Phys. Rev. B* **1988**, *37*, 785–789; c) A. D. Becke, *J. Chem. Phys.* **1993**, *98*, 5648–5652; d) P. J. Stephens, F. J. Devlin, C. F. Chabalowski, M. J. Frisch, *J. Phys. Chem.* **1994**, *98*, 11623–11627.

[61] T. Yanai, D. P. Tew, N. C. Handy, *Chem. Phys. Lett.* **2004**, *393*, 51–57.

[62] Y. Zhao, D. G. Truhlar, *Theor. Chem. Acc.* **2008**, *120*, 215–241.

[63] a) C. Riplinger, P. Pinski, U. Becker, E. F. Valeev, F. Neese, *J. Chem. Phys.* **2016**, *144*, 024109; b) R. Berraud-Pache, F. Neese, G. Bistoni, R. Izsák, *J. Chem. Theory Comput.* **2020**, *16*, 564–575; c) M. Nooijen, R. J. Bartlett, *J. Chem. Phys.* **1997**, *106*, 6441–6448; d) C. Riplinger, F. Neese, *J. Chem. Phys.* **2013**, *138*, 034106; e) C. Riplinger, B. Sandhoefer, A. Hansen, F. Neese, *J. Chem. Phys.* **2013**, *139*, 134101.

RESEARCH ARTICLE

Entry for the Table of Contents
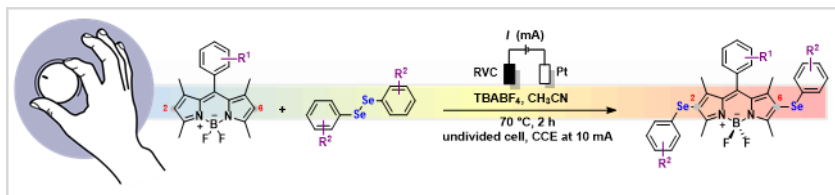
The synthesis of red-emitting BODIPY derivatives through a mild electrochemical diselenation process is reported. The study encompasses substrate scope exploration, photophysical characterization, computational analysis, and the demonstration of their potential as emission-tunable fluorescent probes with large Stokes shift for lipid droplet visualization, offering broad-ranging applications in bioimaging and related fields.